Single-Crystal Raman Spectroscopy of the Rubidium Alums $RbM^{III}(SO_4)_2 \cdot 12H_2O$ (M^{III} = Al, Ga, In, Ti, V, Cr, Fe) between 275 and 1200 cm^{-1}: Correlation between the Electronic Structure of the Tervalent Cation and Structural Abnormalities

Philip L. W. Tregenna-Piggott[†] and Stephen P. Best*[,‡]

Department of Chemistry, University College London, 20 Gordon Street, London WC1H OAJ, U.K.

Received March 15, 1996[⊗]

Low-temperature single-crystal Raman spectra for $RbM^{III}(SO_4)_2 \cdot 12H_2O$ (M^{III} = Al, Ga, In, Ti, V, Cr, Fe) and $RbM^{III}(SO_4)_2 \cdot 12D_2O$ (M^{III} = Al, V) have been collected and assigned in the range 275−1200 cm^{-1}. These results permit classification of the Ti and V rubidium sulfate alums to the β modification, whereas the remaining tervalent cations give the expected α modification. The dimorphism of the rubidium sulfate alums is explained in terms of the electronic structure of the tervalent cation, where the observation of the β modification is associated with unequal occupancy of the t_{2g} (O_h) orbitals. For the rubidium vanadium alums the $^3E_g \leftarrow {}^3A_g$ electronic Raman (eR) transition permits quantification of the trigonal field splitting of the t_{2g} (O_h) orbitals (*ca.* 1940 cm^{-1}). The profile of the eR band is sensitive both to changes in temperature and to deuteration. Analysis of the eR band profile suggests a reduced spin−orbit splitting of the ^3E_g manifold, this being ascribed to excited state Jahn−Teller (J−T) effects. The similarity of the Raman spectra of the cesium and rubidium titanium sulfate alums suggest that they exhibit closely related structural chemistry, with both subject to phase transitions below 80 K. The observation that modes of E_g symmetry are coupled to the structural change is consistent with the interpretation that the trigonal field leaves an orbital doublet ground term for titanium(III), leading to a cooperative J−T effect.

Introduction

Despite being the archetypal ligand, water has proved to be one of the most difficult to treat using ligand field theory. This is due to variability in the balance between the metal−ligand σ and π interactions and the anisotropy of the π interaction in and normal to the plane of the water.[1,2] It is clear that the stereochemistry of coordinated water will impact upon the character of the metal−water interaction; for example, the π donor ability of water will be sensitive to whether the coordination geometry about the oxygen atom is trigonal planar or trigonal pyramidal. While these factors may result in preferred stereochemistries for isolated $[M(OH_2)_6]^{n+}$ species, in condensed media hydrogen bonding interactions are generally considered to dominate. It has been our contention that microscopic aspects of the metal−water interaction are of sufficient magnitude to perturb the molecular structure of metal hydrates and that these interactions may result in unusual structural chemistry or electronic properties of the metal complex.[3−5] An example of this interplay between structural and electronic effects is provided by the dimorphism of the rubidium sulfate alums, $RbM^{III}(SO_4)_2 \cdot 12H_2O$. The adoption of the α or β structural modification, which differ in terms of the stereochemistry of the water molecule coordinated to M^{III},[6] depends on the electronic structure and not the size of the tervalent cation. Only metal cations with unequal occupancy of the t_{2g} (O_h) orbitals give rubidium sulfate β alums; similar structural chemistry is suggested for the corresponding potassium and ammonium alums.[7] This classification of the rubidium alums is based on the crystal habit,[7] this being supported by a limited number of X-ray structure determinations (M^{III} = Al,[8] Cr,[9] and V [5]). We report polarized, low-temperature single-crystal Raman spectra of the rubidium sulfate alums of Al, Ga, In, Ti, V, Cr, and Fe. These results permit the assignment of the Raman-active phonon modes, unambiguous classification of the alum type, and identification of cases of structural instability. For vanadium(III), details of the low-lying electronic structure of the tervalent cation are obtained from analysis of the electronic Raman (eR) transition corresponding to the "intra-t_{2g}" transition, $^3E_g \leftarrow {}^3A_g$.

Experimental Section

The rubidium sulfate alums were prepared by methods analogous to those of the corresponding cesium alums.[10,11] The higher solubilities of the rubidium over the cesium salts leads to increased problems associated with exposure to air (M^{III} = Ti, V) and deliquescence (M^{III} = In). In the case of the rubidium indium sulfate alum it is necessary to prepare and recrystallize the salt from sulfuric acid solutions (1 mol dm^{-3}) containing an excess of rubidium sulfate. Deuterated samples were prepared by repeated recrystallization (at least 3 times) from

* Author to whom correspondence should be addressed.
[†] Current address: Department of Physics, Monash University, Wellington Rd, Clayton, Victoria, 3168, Australia.
[‡] Current address: School of Chemistry, University of Melbourne, Parkville 3052, Victoria, Australia.
[⊗] Abstract published in *Advance ACS Abstracts,* August 15, 1996.

(1) Bencini, A.; Benelli, C.; Gatteschi, D. *Coord. Chem. Rev.* **1984**, *60*, 131−169.
(2) Stranger, R.; Sirat, K.; Smith, P. W.; Grey, I. E.; Madsen, I. C. *J. Chem. Soc., Dalton Trans*. **1988**, 2245−2253.
(3) Best, S. P.; Forsyth, J. B. *J. Chem. Soc., Dalton Trans*. **1991**, 1721−1725.
(4) Best, S. P.; Forsyth, J. B.; Tregenna-Piggott, P. L. W. *J. Chem. Soc., Dalton Trans*. **1993**, 2711−2715.
(5) Beattie, J. K.; Best, S. P.; Del Favero, P.; Skelton, B. W.; Sobolev, A. N.; White; A. H. *J. Chem. Soc., Dalton Trans*. **1996**, 1481−1486.
(6) Best, S. P.; Forsyth, J. B. *J. Chem. Soc., Dalton Trans*. **1990**, 395−400.
(7) Haussühl, S. *Z. Kristallogr., Kristallgeom., Kristallphys., Kristallchem.* **1961**, 116, 371−405.
(8) Larson, A. C.; Cromer, D. T. *Acta Crystallogr*. **1967**, *22*, 793−800.
(9) Ledsham, A. H. C.; Steeple, H. *Acta Crystallogr.* **1969**, *B25*, 398−400.
(10) Best, S. P.; Beattie, J. K.; Armstrong, R. S. *J. Chem. Soc., Dalton Trans*. **1982**, 1655−1664.
(11) Best, S. P.; Beattie, J. K.; Armstrong, R. S. *J. Chem. Soc., Dalton Trans*. **1984**, 2611−2624.

S0020-1669(96)00275-3 CCC: $12.00

sulfuric acid-$^2H_2$ (1 mol dm^{-3}, 99.5 at. % ^{2}H), whereupon the sample was estimated to be at least 98% substituted; this estimate was confirmed by the ratio ν(OH)/ν(OD). Large single crystals were prepared by a method described in the literature.[11]

The factor group analysis (FGA) of the alums has previously been published;[10,12] this is the same for α and β alums and is independent of the identity of the monovalent cation in the lattice. Scattering experiments of the type $X'(\alpha\beta)Y'$, where X' and Y' are related to the crystallographic X and Y directions by a rotation by $\pi/4$ about Z and $\alpha\beta$ is the component of the polarizability tensor under examination, were conducted. In these experiments $A_g + E_g$ modes are active when $\alpha\beta = ZZ$; E_g, when $\alpha\beta = Y'X'$; and F_g, when $\alpha\beta = ZX'$ or $Y'Z$.[10] Faces of the type [110] corresponding to the incident and exit directions of the laser, and [$\bar{1}$10], the collection direction for the scattered radiation, were cut using a diamond saw and polished using 1 μm diamond paste (Hyprez). Epoxy glue (Araldite Rapid) was used to attach the crystal to a three-circle goniometer head which was placed in the sample space of an Oxford Instruments MD4 cryostat. Heat exchange between the crystal and the cryostat was effected by *ca.* 0.1 bar of helium exchange gas. The temperature of the sample was estimated from the relative intensities of the Stokes and anti-Stokes Raman bands or, at liquid helium temperatures, from a Rh/Fe resistor attached to the sample holder. Raman spectra were collected using Spex 1401 or 14018 double monochromators fitted with Burle C31034 GaAs or Hamamatsu R585 bialkali photomultiplier tubes operated in single photon counting mode. Excitation was provided by Coherent Model I 70-4 or I 3000K lasers.

Results

Although detailed studies have been completed for the cesium alums, including a full assignment of the spectra below 1200 cm^{-1},[10,11,13−16] previous single crystal Raman studies of the rubidium alums is limited to room temperature measurements of $RbAl(SO_4)_2{\cdot}12H_2O$.[12] For both the α and β alum modifications the space group symmetry is $Pa\bar{3}$, the mono- and tervalent cations lie on sites of S_6 symmetry, and the anions lie on sites of C_3 symmetry, accordingly, the FGA of α and β alums is equivalent, and the general form of their single-crystal Raman spectra is closely related.[14] Polarized spectra of $RbV(SO_4)_2{\cdot}12H_2O$ in the region 275−1200 are shown in Figure 1. This region of the spectrum contains the internal modes of sulfate and the tervalent hexaaqua cation and the external modes of water coordinated to the mono- and tervalent cations, giving rise to a FGA prediction of $11A_g + 11E_g + 33T_g$ first-order phonon modes. The E_g modes are key to the assignment of the Raman spectra of the alums since these generally give rise to bands of at least moderate intensity, and all modes, except $\nu_1(MO_6)$ and $\nu_1(SO_4)$, have components of E_g symmetry. For the rubidium sulfate alums all 11 of the E_g bands are observed for Al, Ga, Fe, and Ti, and 10 of the E_g bands are observed for In, V, and Cr.

Alum Modification. Previous Raman studies of cesium α and β alums suggest that the T_g components of the $\nu_3(SO_4)$ mode have band profiles which are highly sensitive to the alum type,[17] and these are shown in Figure 2. There is a clear distinction between the spectra of the titanium and vanadium salts compared with those of all other rubidium sulfate alums. The band profile of the $\nu_3(SO_4)$ mode of the rubidium sulfate alums match closely those of either the cesium sulfate α or β alums and confirm the classification of the rubidium titanium and vanadium sulfate alums to the β modification. This classification is in exact agreement with deductions based on the crystal habit[7] and the available crystallographic determinations (Al,[8] Cr,[9] and V[5]). The confirmation of Haüssuhl's classification[7] of the rubidium titanium sulfate alum is important since it establishes the link between the structural chemistry and partial occupancy of the t_{2g} orbitals. There are significant differences in the orientation of the plane of the coordinated water molecule for the α and β structures. For the β alums, the MO bond vector lies within 2° of the plane of the water molecule (trigonal planar coordination about the oxygen atom) and the plane of the water molecule is twisted about the MO bond by 19−23° from T_h toward *all-horizontal* D_{3d} symmetry.[3,4,18] For the α alums the tervalent hexaaqua cation is distorted from T_h symmetry by a tilt of the plane of the water molecule by *ca.* 18° (trigonal pyramidal coordination about the oxygen atom).[6]

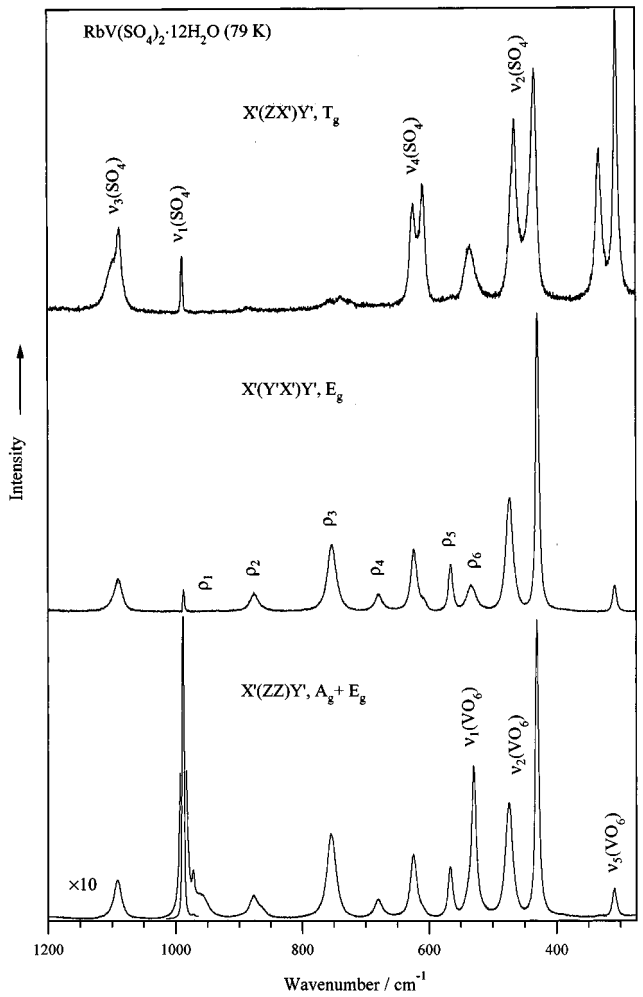

Figure 1. Single-crystal Raman spectra and assignments of $RbV(SO_4)_2{\cdot}12H_2O$: Spectral bandwidth 2.96 cm^{-1} at 600 cm^{-1}; 4 s integration time, step size 0.4 cm^{-1}; 50 mW, 457 nm radiation at sample. Sensitivities: $X'(Y'X')Y'$, 10 220; $X'(ZX')Y'$, 1840; and $X'(ZZ)Y'$, 141 237 counts s^{-1}. For clarity, leakage of strong bands of A_g or T_g symmetry have been removed from the E_g spectrum by subtraction.

Internal Modes of the Tervalent Hexaaqua Cations. The assignment of the internal modes of the tervalent hexaaqua cation are based on the assignments from the cesium sulfate alums,[10,11,13−15] these being confirmed by the shifts observed on deuteration (Table 1). The $\nu_1(MO_6)$ mode gives rise to A_g and T_g components, with the T_g component generally too weak

(12) Eysel, H. H.; Eckert, J. *Z. Anorg. Allg. Chem.* **1976**, 424, 68−80.
(13) Best, S. P.; Beattie, J. K.; Armstrong, R. S.; Braithwaite, G. P. *J. Chem. Soc., Dalton Trans.* **1989**, 1771−1777.
(14) Best, S. P.; Beattie, J. K.; Armstrong, R. S. *J. Chem. Soc., Dalton Trans.* **1992**, 299−304.
(15) Armstrong, R. S.; Beattie, J. K.; Best, S. P.; Cole, B. D.; Tregenna-Piggott, P.L. W. *J. Raman Spectrosc.* **1995**, *26*, 921−927.
(16) Beattie, J. K.; Armstrong, R. S.; Best, S. P. *Spectrochim. Acta* **1996**, *51A*, 539−548.
(17) Armstrong, R. S.; Beattie, J. K.; Best, S. P.; Skelton, B. W.; White, A. H. *J. Chem. Soc., Dalton Trans.* **1983**, 1973−1975.
(18) Best, S. P.; Forsyth, J. B. *J. Chem. Soc., Dalton Trans.* **1990**, 3507−3511.

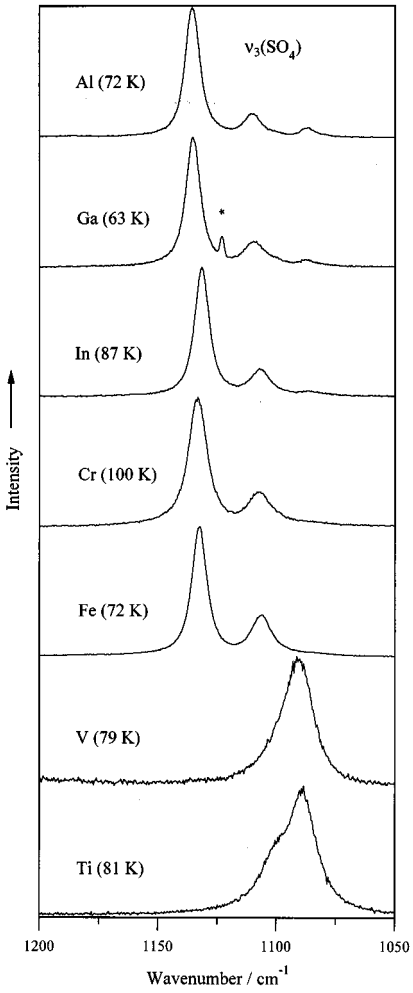

Figure 2. T_g components of the $\nu_3(SO_4)$ mode of the rubidium alums, $RbM(SO_4)_2 \cdot 12H_2O$, M = Al, Ga, In, Cr, Fe, Ti, V. The temperature of the sample is given in parentheses; the asterisk designates an emission due to the room lights.

to permit identification. The low intensity of the T_g component suggests that there is a weak factor group coupling of this mode within the crystal, and the wavenumber of the A_g component reflects the local environment of the tervalent hexaaqua cation. In general there is little change to the wavenumber of the $\nu_1(MO_6)$ mode with a change in alum modification, and the wavenumbers of this mode for the rubidium alums [545 (Al), 538 (Ga), 500 (In), 518 (Ti), 540 (Cr), and 526 cm^{-1} (Fe)] are within experimental error of those obtained for the corresponding cesium sulfate alums.[10,11] For the rubidium vanadium alum the $\nu_1(VO_6)$ mode is observed at 531 cm^{-1}, shifting to 508 cm^{-1} on deuteration [$\nu_D/\nu_H = 0.96$, ν_D/ν_H (calc) $= \sqrt{(18/20)} = 0.95$]. The value of $\nu_1(VO_6)$ is 6 cm^{-1} higher for the rubidium than the corresponding cesium alum. This difference is surprisingly large given that there is no change in alum modification and the V−O bond lengths for the cesium and rubidium vanadium alums are not significantly different [1.992(1) {Cs} and 1.996(3) {Rb}].[5]

The $\nu_2(MO_6)$ and $\nu_2(SO_4)$ modes occupy the spectral region 400−500 cm^{-1}, and both give rise to $E_g + 2T_g$ Raman-active modes. The profiles and wavenumbers of the E_g bands in the spectra of the rubidium alums suggest that there is significant coupling between the $\nu_2(MO_6)$ and $\nu_2(SO_4)$ modes, with the magnitude of the coupling highly sensitive to the wavenumber of $\nu_2(MO_6)$ (Figure 3). For the cesium sulfate α alums of Co,[14] Rh,[13] and Ir,[14] the high-wavenumber $\nu_2(MO_6)$ mode is only weakly coupled with $\nu_2(SO_4)$ and the wavenumbers and band profiles of the $\nu_2(SO_4)$ modes are similar. Further, the band profile and wavenumber of the $\nu_2(SO_4)$ mode of $RbCr(SO_4)_2 \cdot 12H_2O$ closely matches that found for the cesium sulfate α alums, suggesting that the E_g bands found at 503 and 447 cm^{-1} in $RbCr(SO_4)_2 \cdot 12H_2O$ may be assigned to the "uncoupled" components of the $\nu_2(CrO_6)$ and $\nu_2(SO_4)$ modes, respectively. For the remaining rubidium alums the spectral features are consistent with significant coupling between the $\nu_2(MO_6)$ and $\nu_2(SO_4)$ modes. Uncoupled wavenumbers for the $\nu_2(MO_6)$ mode are estimated by subtracting the uncoupled $\nu_2(SO_4)$ wavenumber (447 cm^{-1}) from the sum of the E_g components of the coupled $\nu_2(MO_6)$ and $\nu_2(SO_4)$ modes. Accordingly, uncoupled $\nu_2(MO_6)$ wavenumbers are estimated to be 466 (Al), 450 (Ga), 443 (In), 461 (Ti), 459 (V), and 458 cm^{-1} (Fe), in close agreement with similar estimates of the uncoupled $\nu_2(MO_6)$ mode in the cesium β alums (464, 450, 444, 459, 454, and 456 cm^{-1}, respectively[10,11]). The similarity of values of $\nu_1(MO_6)$ and $\nu_2(MO_6)$ for the cesium and rubidium alums suggests that the metal−water stretching modes are insensitive to the changes in the coordination geometry which accompany the change in alum type.

The $\nu_5(MO_6)$ mode gives rise to $A_g + E_g + 3T_g$ bands which are well-separated from other modes of the crystal (Figure 1). The band profiles and wavenumbers of this mode are sensitive to the identity of the tervalent cation and to the alum type (Table 1). The average of the shifts observed on deuteration (ν_D/ν_H of 0.95 (Al) and 0.95 (V)) are in agreement with calculation (0.95).

Internal Modes of Sulfate. The wavenumbers and band profiles of the internal modes of sulfate are sensitive to the alum type. The intense A_g bands assigned to $\nu_1(SO_4)$ occur at 992 ± 1 cm^{-1} for the corresponding α alums[13,14] and 988 ± 1 cm^{-1} for the β alums,[10,11,15] with weaker satellite bands due to $\nu_1(S^{16}O_3{}^{18}O)$ at 977 ± 1 and 971 ± 1 cm^{-1}, respectively. For the hydrates the $\nu_3(SO_4)$ mode occurs at *ca.* 1100 cm^{-1}, is well-separated from other modes in the spectrum, and has a profile which is characteristic of the alum type (Figure 2). The $\nu_2(SO_4)$ is involved in coupling with $\nu_2(MO_6)$ as discussed above. The $\nu_4(SO_4)$ mode gives rise to bands at ca. 640 cm^{-1}, with an external mode of coordinated water lying close by. The E_g components of the two modes have wavenumber and intensity changes which indicate significant coupling in the case where M^{III} = Al, Ga, and Fe (Figure 3). It is also apparent that the relative intensity of the E_g component of $\nu_4(SO_4)$ is appreciably greater for α than β alums.

External Modes of Coordinated Water. The external (or librational) modes of water correspond to hindered rotations of the molecule about its three principal axes. There are three external modes for each of the two crystallographically distinct water molecules in the unit cell, and each of the external modes of water gives rise to $A_g + E_g + 3T_g$ Raman-active components. Since all of the E_g bands can be accounted for in the spectra, the external modes of coordinated water are assigned with reference to their E_g components. The T_g and A_g components (when observed) are assigned on the basis of their proximity to the E_g component. Assignments made on this basis are supported by the magnitude of the shifts observed on deuteration (Table 1). The six external modes are labeled $\rho_1-\rho_6$ in order of decreasing wavenumber. The X-ray[5,8,9,19] and neutron[3,4,6,18] diffraction structures of the alums show that the hydrogen bonds which involve the water molecule coordinated to metal(III) are the strongest in the lattice and are therefore likely to give rise to the external modes of highest wavenumber ($\rho_1-\rho_3$). For the

(19) Beattie, J. K.; Best, S. P.; Skelton, B. W.; White, A. H. *J. Chem. Soc., Dalton Trans.* **1981**, 2105−2111.

Table 1. Band Wavenumbers (cm^{-1}) and Assignments between 275 and 1200 cm^{-1} of Spectra of the Rubidium Sulfate Alums, $RbM^{III}(SO_4)_2 \cdot 12Y_2O$[a]

		AlH	AlD	ν(D)/ν(H)	GaH	InH	CrH	FeH	TiH	VH	VD	ν(D)/ν(H)
	A_g				326 (vw)	305 (w)	316 (w)	316 (w)				
$\nu_5(MO_6)$	E_g	336 (m)	317 (w)	0.94	319 (w)	294 (w)	308 (w)	306 (m)	294 (w)	311 (w)	295 (w)	0.95
	T_g	338 (m)	323 (m)	0.96	317 (sh)	294 (m)	309 (m)	304 (s)	292 (m)	306 (s)	292 (s)	0.95
	T_g	354 (w)	334 (w)	0.94	320 (m)	297 (sh)	312 (sh)	310 (s)	324 (m)	333 (s)	318 (m)	0.95
	T_g				338 (w)	318 (w)	330 (w)	330 (w)				
$\nu_2(SO_4)$[b]	E_g	440 (s)	467 (s)	1.06	432 (m)	464 (s)	447 (m)	436 (m)	435 (m)	431 (s)	469 (m)	1.09
	T_g	441 (s)	466 (s)	1.06	432 (m)	457 (s)	449 (m)	435 (m)	441 (s)	434 (s)	458 (sh)	1.06
	T_g	460 (s)	473 (sh)	1.03	450 (sh)	461 (s)	458 (m)				462 (s)	
$\nu_2(MO_6)$[b]	E_g	473 (s)	413 (w)	0.87	465 (m)	426 (w)	503 (m)	470 (m)	473 (m)	475 (m)	410 (s)	0.86
	T_g	471 (m)	424 (m)	0.90	461 (s)	424 (m)	504 (sh)	460 (m)	463 (m)	465 (s)	413 (m)	0.89
	T_g				465 (sh)	442 (sh)		468 (sh)				
	A_g		351 (w)			474 (sh)						
ρ_6	E_g	518 (m)	371 (m)	0.72	519 (w)		520 (sh)	513 (vw)	536 (m)	533 (m)	387 (w)	0.73
	T_g		350 (w)		517 (sh)	494 (m)	520 (m)	515 (m)	536 (m)	535 (m)	403 (m)	0.75
	T_g	516 (sh)	376 (m)	0.73	522 (m)	529 (m)		530 (m)				
	T_g	523 (s)						543 (sh)				
$\nu_1(MO_6)$	A_g	545 (m)	519 (m)	0.95	538 (s)	500 (s)	540 (s)	526 (vs)	518 (m)	531 (s)	508 (m)	0.96
	T_g						545 (sh)				507 (vw)	
	A_g										414 (vw)	
ρ_5	E_g	599 (s)	447 (m)	0.75	594 (s)	585 (m)	592 (m)	594 (s)	570 (m)	568 (m)	416 (sh)	0.73
	T_g	608 (s)	438 (m)	0.72	604 (w)	582 (w)		604 (w)	575 (sh)		430 (w)	
	T_g	615 (s)	447 (w)	0.73	617 (s)							
	T_g											
	A_g											
$\nu_4(SO_4)$	E_g	639 (s)	636 (s)	1.00	633 (m)	625 (s)	631 (s)	632 (s)	625 (m)	626 (m)	630 (w)	1.01
	T_g	623 (s)	636 (m)	1.02	632 (w)	609 (s)	616 (m)	616 (s)	607 (m)	609 (m)		
	T_g	639 (w)	643 (m)	1.01	645 (sh)	618 (sh)	635 (sh)	641 (w)	623 (m)	624 (m)	621 (m)	1.00
	T_g					635 (w)						
	A_g										485 (w)	
ρ_4	E_g	714 (s)	532 (m)	0.75	708 (m)	701 (m)	701 (m)	705 (m)	677 (m)	681 (w)	500 (w)	0.73
	T_g	712 (w)	519 (w)	0.73	704 (w)	691 (w)	698 (w)	701 (w)	675 (w)		507 (vw)	
	T_g	729 (w)					726 (w)					
	T_g											
	A_g	789 (w)							755 (m)	755 (w)	548 (w)	0.73
ρ_3	E_g	781 (w)	555 (s)	0.71	776 (w)	775 (w)	774 (w)	779 (w)	797 (vw)	755 (m)	531 (m)	0.70
	T_g	785 (w)	556 (m)	0.71	777 (w)	779 (w)	753 (sh)	783 (w)	724 (vw)	722 (sh)	532 (w)	0.74
	T_g						780 (w)		763 (vw)	739 (w)		
	T_g									755 (w)	546 (w)	0.72
	A_g	875 (w)			872 (w)		872 (w)	862 (w)	854 (sh)	865 (w)	650 (w)	0.75
ρ_2	E_g	891 (w)	655 (w)	0.74	898 (w)	894 (w)	896 (w)	879 (w)	866 (w)	878 (w)	653 (m)	0.74
	T_g	869 (m)			866 (w)	864 (w)	864 (w)	855 (w)	872 (vw)	884 (w)	646 (m)	0.73
	T_g	893 (m)	653 (sh)	0.73	887 (sh)	893 (w)	893 (w)	880 (w)			659 (m)	
	T_g				898 (w)							
	A_g							941 (w)	961 (sh)	961 (w)	697 (w)	0.73
ρ_1	E_g	940 (m)	697 (m)	0.74	933 (m)	923 (m)	932 (w)	930 (w)	932 (vw)		694 (w)	
	T_g	935 (vw)	695 (vw)	0.74			929 (sh)			922 (vw)	682 (vw)	0.74
	T_g									958 (vw)	702 (w)	0.73
	T_g											
$\nu_1(S^{16}O^{18}O_3)$	A_g	977 (m)	976 (m)	1.00	977 (m)	976 (m)	976 (m)	976 (m)	972 (m)	973 (m)	971 (m)	1.00
$\nu_1(SO_4)$	A_g	992 (vvs)	991 (vvs)	1.00	993 (vvs)	992 (vvs)	992 (vvs)	991 (vvs)	988 (vvs)	989 (vvs)	988 (vvs)	1.00
	T_g											
	A_g											
$\nu_3(SO_4)$	E_g	1100 (s)	1111 (m)	1.01	1100 (m)	1098 (m)	1098 (m)	1096 (m)	1092 (w)	1092 (m)	1102 (w)	1.01
	T_g	1087 (w)	1101 (sh)	1.01	1087 (w)	1086 (w)	1082 (sh)	1083 (sh)	1088 (m)	1088 (m)	1099 (m)	1.01
	T_g	1110 (m)	1110 (sh)	1.00	1109 (m)	1107 (m)	1107 (m)	1106 (m)	1100 (w)	1101 (w)	1099(sh)	1.00
	T_g	1136 (s)	1136 (s)	1.00	1135 (s)	1132 (s)	1133 (s)	1132 (s)	1112 (sh)	1130 (sh)	1128 (sh)	1.00

[a] The alums are designated by the identity of M^{III} and *Y*. sh = shoulder, vw = very weak, w = weak, m = medium, s = strong, vvs = very very strong. [b] Strong coupling between $\nu_2(SO_4)$ and $\nu_2(MO_6)$. The values of ν_D/ν_H listed for these modes are strongly perturbed by coupling, where $\nu_2(MO_6) > \nu_2(SO_4)$ for the hydrate but $\nu_2(MO_6) < \nu_2(SO_4)$ for the deuterate.

cesium sulfate and selenate alums ρ_1 has been assigned to the rocking motion, ρ_2 to the twisting motion, and ρ_3 to the wagging motion of the water molecule coordinated to M^{III} on the basis of the sensitivity of the wavenumbers of the external modes to $r(M^{III}-O)$ and the alum type.[14] No attempt has been made to order the external modes of the monovalent cation.

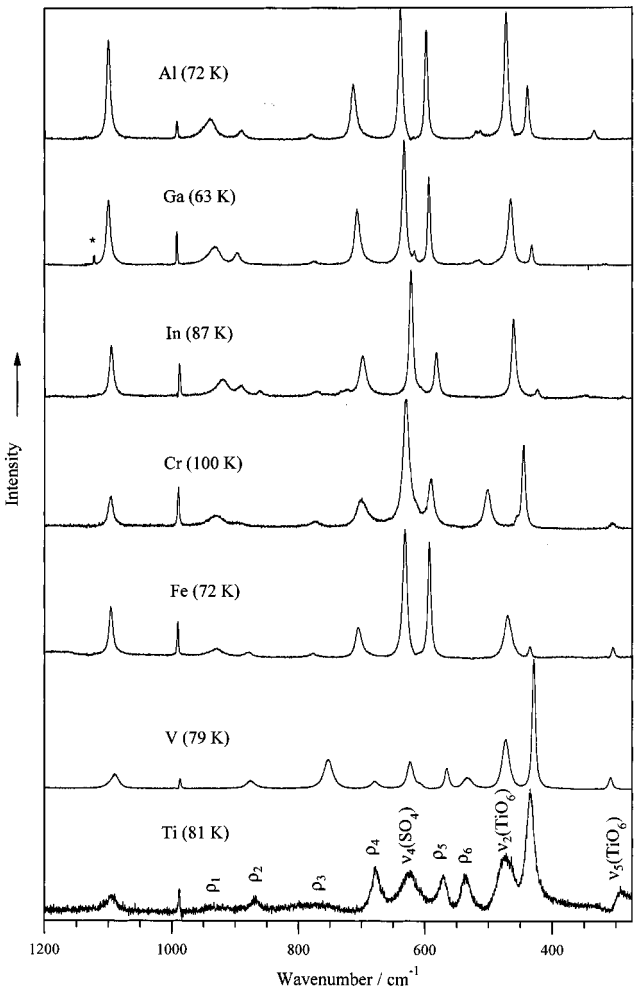

Figure 3. E_g Raman spectra of rubidium alums, $RbM(SO_4)_2{\cdot}12H_2O$. For clarity, leakage of strong bands of A_g or T_g symmetry have been removed from the spectra by subtraction; the asterisk designates an emission due to the room lights.

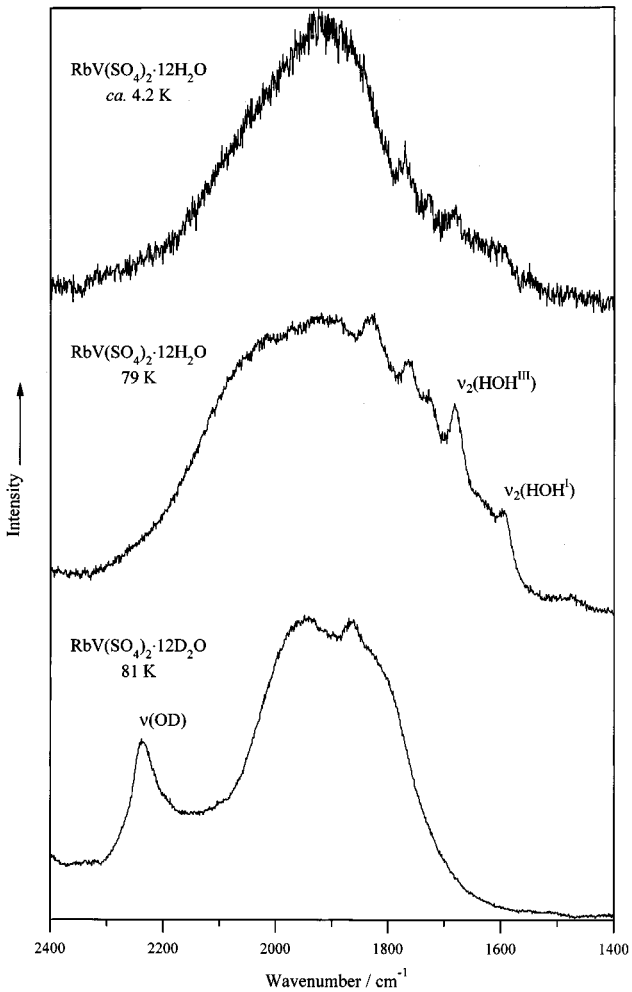

Figure 4. Electronic Raman bands of $RbV(SO_4)_2{\cdot}12H_2O$ and $RbV(SO_4)_2{\cdot}12D_2O$. Assignment of the bands which are due to the bending modes of water coordinated to the monovalent and tervalent cation, designated by $\nu_2(HOH^I)$ and $\nu_2(HOH^{III})$, respectively, are based on ref 24. Assignment of the stretching mode of coordinated D_2O, ν(OD), is supported by comparison of the spectra of the corresponding aluminium alums.

Phase Transition in $RbTi(SO_4)_2{\cdot}12H_2O$. The spectra of $RbTi(SO_4)_2{\cdot}12H_2O$ are analogous to those of the corresponding cesium alum,[11] both being characterized by the unusually broad and distorted profiles of a number of bands in the spectrum, this is particularly pronounced for the bands arising from modes of E_g symmetry (Figure 3). The ρ_1 and ρ_3 external modes of water coordinated to Ti^{III} are most markedly affected, and their band profiles are distinguished with difficulty from the baseline. Behavior of this sort is commonly associated with dynamic disorder of the water molecules.[20−22] The $\nu_5(TiO_6)$ and $\nu_2(TiO_6)$ modes also exhibit significant distortion of their band profiles. In contrast, the A_g and T_g components of the modes which give broad and distorted E_g components have profiles which are comparable with those found for the corresponding vanadium alum. These observations together with the presence of an intense low-wavenumber mode which moves to lower wavenumber on cooling are indicative of the onset of a phase transition. Recent neutron powder diffraction studies of $CsTi(SO_4)_2{\cdot}12D_2O$ indicate that the salt exists in high-temperature cubic and low-temperature orthorhombic phases, with a phase transition temperature between 9 and 12 K.[23] The similarities of the temperature dependence of the Raman spectra of the rubidium and cesium titanium sulfate alums suggest that similar structural chemistry occurs for both alums.

Electronic Raman Band of $[V(OH_2)_6]^{3+}$. The cesium and ammonium vanadium alums have been found to exhibit a broad band centered on 1940 cm^{-1}, which has been assigned to an electronic transition between the trigonally split components of the $^3T_{1g}$ (O_h) ground term of the hexaaqua vanadium(III) ion.[24] For $RbV(SO_4)_2{\cdot}12H_2O$ a band of E_g polarization, centered on 1940 cm^{-1}, is apparent in the spectrum, and this is assigned to the $^3E_g \leftarrow {}^3A_g$ (S_6) eR transition. The band profile is sensitive to temperature, with high- and low-wavenumber components losing intensity on cooling to 4 K (Figure 4). The broad band attributed to the eR transition is accompanied by a number of features with half-widths similar to those of vibrational bands. These latter features are due to the ν_2(HOH) mode and to a range of combination and overtone bands. It is interesting that the intensities of the E_g components of these modes are much greater in the spectra of the vanadium alums than of the corresponding salts of other tervalent cations. On deuteration there is a marked change in the profile of the band assigned to the eR transition, this being dominated by components at *ca.*

(20) Tanaka, H.; Henning, J. H.; Lutz, D.; Kliche, G. *Spectrochim. Acta* **1987**, *43A*, 395.
(21) Eckers, W.; Lutz, H. D. *Spectrochim. Acta* **1985**, *41A*, 1321.
(22) Frindi, M.; Peyrard, M.; Remoissenet, M. *J. Phys.* **1980**, *C13*, 3493.
(23) Tregenna-Piggott, P. L. W.; Best, S. P.; O'Brien, M. C. M.; Knight, K. S.; Forsyth, J. B.; Pilbrow, J. Manuscript in preparation.
(24) Best, S. P.; Clark, R. J. H. *Chem. Phys. Lett.* **1985**, 122, 401−405.

1973 and 1828 cm^{-1} with half-widths of *ca*. 160 cm^{-1}, with an additional band at 2240 cm^{-1} which is assigned to an O−D stretching mode (Figure 4). The vibrational bands on the low-wavenumber side of the eR band of the hydrate shift to give a broad unstructured band at 1200 cm^{-1} on deuteration.

Discussion

The structural and spectroscopic characteristics of the rubidium sulfate alums are in close agreement when M^{III} is a group 13 cation or a transition metal cation with equal occupancy of the metal(III) t_{2g} (O_h) orbitals. In these cases there is a change of alum modification with exchange of rubidium by the larger cesium cation, and this results in a change in the conformation of the water molecule coordinated to the tervalent cation. There is no evidence that this change in water coordination geometry affects significantly $r(M^{III}-O)$ or the vibrational frequencies of the $M^{III}-O$ stretching modes. However, for titanium(III) and vanadium(III), where there is unequal occupancy of the metal(III) t_{2g} (O_h) orbitals, the β modification is adopted with all monovalent cations. Since the sizes of the group 13 cations encompasses those of titanium(III) and vanadium(III), the different structural chemistry must result from a preferred orientation of the coordinated water molecule. The principle interactions which can act to lift the orbital degeneracy resulting from partial occupancy of the t_{2g} (O_h) orbitals in the alum lattice are the trigonal field splitting associated with the S_6 site symmetry and Jahn−Teller (J−T) and spin−orbit (SO) coupling. The splitting of the $^3T_{2g}$ ground term of vanadium(III) is considerable, based on the wavenumber of the $^3E_g \leftarrow {}^3A_g$ electronic Raman band, the electronic spectra,[25] and magnetochemistry,[26] and this has been interpreted in terms of the trigonal field splitting being the predominant interaction. Luminescence measurements of the $^2E_g \rightarrow {}^4A_{2g}$ transition of chromium(III) doped into α and β alum lattices suggest that the magnitude of the trigonal field splitting is significantly larger for β alums than α alums.[27] This difference in the magnitude of the trigonal field at the M^{III} site in the α and β alum structures underlies the preferred adoption of the β modification by tervalent cations with unequal occupancy of the t_{2g} (O_h) orbitals.

The difference in the trigonal field at the M^{III} site of the α and β alums must be explained in terms of metal−water π bonding interactions since the $O-M^{III}-O$ bond angles are similar for the two alum modifications and are little distorted from octahedral. The anisotropy of the M−L π interaction in and normal to the plane of the water molecule together with its orientation relative to the MO_6 framework dominate the trigonal field.[3] For the α alums, the trigonal pyramidal coordination geometry about the oxygen atom reduces its ability to engage in π bonding and the alignment of the planes of the water molecules with the MO_6 framework contributes to a small trigonal field splitting. For the β alums, the coordination geometry about the oxygen is trigonal planar, ideal for $p\pi-d\pi$ bonding. Further, the maximum splitting of the energies of the t_{2g} orbitals is obtained when the plane of the water molecule is inclined by 45° to the MO_6 framework (giving effective D_{3d} symmetry for an ion lying on the S_6 site). Within the β alum structure the water molecule is inclined by between 19 and 22° toward *all-horizontal* D_{3d} symmetry.[3,4] This arrangement is a compromise between the hydrogen-bonding constraints of the lattice and the electronic considerations of the ion. If the metal−water π interaction is greater normal to the plane of the water molecule, as is demonstrated most clearly in polarized neutron diffraction measurements of $CsMo(SO_4)_2\cdot 12D_2O$,[28] then this orientation of the coordinated water molecule will lead to a splitting of the energies of the t_{2g} (O_h) orbitals so as to give $e_g < a_g$ (S_6). For a d^2 ion such as vanadium(III) this leads to an orbitally non-degenerate ground term, a conclusion supported by analysis of the magnetochemistry.[26,29] It follows that for the d^1 ion, titanium(III), the trigonal field splitting leaves a ground term with 2-fold orbital degeneracy, hence, the trigonal field of the β alums distorts the complex toward a local rather than a global electronic minimum. The orbitally degenerate ground term will be subject to J−T and SO coupling. Magnetochemical measurements of the titanium alums indicate a quenching of the SO coupling, which suggests that the J−T coupling is dominant.[37] We suggest that J−T coupling, in a cooperative form, is implicated in the phase transition below 15 K. The orbital degeneracy of the ground term (E_g) may only be lifted by coupling to vibrational modes of E_g symmetry. The pronounced broadening of the E_g bands of $RbTi(SO_4)_2\cdot 12H_2O$ (Figure 3), particularly the components of the external modes of water coordinated to titanium(III) and to the internal modes of TiO_6, is consistent with this interpretation. The inference that the E_g trigonal term constitutes the ground term of $[Ti(OH_2)_6]^{3+}$ is at variance with current interpretations of the magnetochemistry and EPR spectroscopy of $CsTi(SO_4)_2\cdot 12H_2O$[30,31] but is consistent with the interpretation of the EPR spectra of methanolic solutions of Ti^{3+}(aq).[32] We note that the interpretation of the electronic structure of the titanium(III) cation within the alum lattice has been based on the assumption that the trigonal site symmetry is retained to liquid helium temperatures.[33−37] This assumption is clearly invalid, and a reinvestigation of the magnetism and EPR of titanium(III) in the β alum lattice is in progress.[23,38]

The profile of the eR band of vanadium(III) in the rubidium and cesium β alum lattice is similar but is highly sensitive both to deuteration and temperature (Figure 4). The energy levels arising from the ^3T_g (T_h) term as a result of perturbations due to the trigonal field and SO coupling are calculated using expressions given in ref 39 and are shown in Figure 5. The electronic transition is E_g polarized so that transitions of the type $\hat{A}_g \leftrightarrow \hat{E}_g$ or $\hat{E}_g \leftrightarrow \hat{E}_g$ are allowed. Lowering the temperature from 80 to 4.2 K will result in an increase in the intensity of the bands involving excitation from $1\hat{A}_g$ by a factor of 1.7 relative to the phonon modes of the spectrum and a factor of 8.6 relative to eR bands involving excitation from $1\hat{E}_g$ (assuming Boltzmann populations). The effect of temperature on the eR band (Figure 4) is to reduce intensity from both high- and low-wavenumber components. As is evident from Figure

(25) Hitchman, M. A.; McDonald, R. G.; Smith, P. W.; Stranger, R. *J. Chem. Soc., Dalton Trans.* **1988**, 1393−1395.
(26) Figgis, B. N.; Lewis, J.; Mabbs, F. E. *J. Chem. Soc.* **1960**, 2480.
(27) Berry, A. J.; Armstrong, R. S.; Cole, B. D.; Nugent, K. W. *J. Chem. Soc., Dalton Trans*., submitted for publication.
(28) Best, S. P.; Figgis, B. N.; Forsyth, J. B.; Reynolds, P. A.; Tregenna-Piggott, P. L. W. *Inorg. Chem.* **1995**, *34*, 4605−4610.
(29) Fritz, J. J.; Pinch, H. L. *J. Am. Chem. Soc.* **1956**, *78*, 6223−6225.
(30) Jesion, A.; Shing, Y. H.; Walsh, D. In *Proceedings of the Eighteenth Colloques Ampere*, Nottingham, England, 9−14 Sept 1974; Andrew, E. R., Bates, C. A., Eds.; University of Nottingham Press: Nottingham, England, 1974; p 561.
(31) Tachikawa, H.; Murakami, A. *J. Phys. Chem.* **1995**, *99*, 11046−11050.
(32) Tachikawa, H.; Ichikawa, T.; Yoshida, H. *J. Am. Chem. Soc.* **1990**, *112*, 977−981.
(33) Rumin, N.; Vincent, C.; Walsh, D. *Phys. Rev. B* **1973**, *7*, 1811−1816.
(34) Shing, Y. H.; Walsh, D. *Phys. Rev. Lett.* **1974**, *33*, 1067−1069.
(35) MacKinnon, J. A.; Bickerton, J. L. *Can. J. Phys.* **1970**, *48*, 814−818.
(36) Benzie, R. J.; Cooke, A. H. *Proc. R. Soc. London, A* **1951**, *209*, 269−278.
(37) Figgis, B. N.; Lewis, J.; Mabbs, F. *J. Chem. Soc.* **1963**, 2473.
(38) Best, S. P.; O'Brien, M. C. M.; Pilbrow, J.; Tregenna-Piggott, P. L. W. Work in progress.
(39) Mabbs, F. E.; Machin, D. J. *Magnetism and Transition Metal Complexes*; Chapman and Hall: London, 1973.

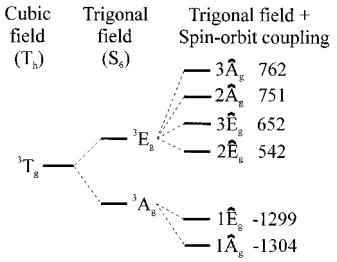

Figure 5. Splitting of the ^3T_g term of $[V(OH_2)_6]^{3+}$ by trigonal field and spin−orbit coupling. Energies (cm^{-1}) were calculated using expressions obtained from treating the trigonal field and spin−orbit coupling as simultaneous perturbations to the ^3T_g (T_h) term.[37] The trigonal field parameter was set to +1940 cm^{-1}, and the product λA, where A depends on $10Dq$ and B, was adjusted to give a splitting between $1\hat{A}_g$ and $1\hat{E}_g$ of 4.95 cm^{-1}, a value deduced from magnetochemical measurements.[29]

5 the high-wavenumber side of the eR band is comprised of transitions to $2\hat{A}_g$ and $3\hat{A}_g$; these occur only from $1\hat{E}_g$, and the loss of intensity from the high-wavenumber range of the eR band reflects the depopulation of $1\hat{E}_g$ on cooling. The loss of intensity from the lower wavenumber portion of the eR band on cooling may suggest assignment to transitions from $1\hat{E}_g$ or to phonon modes. The latter interpretation is supported by the narrow half-widths of the bands contributing to the low-wavenumber tail of the eR band, with these features assigned to bending modes of water and to combination tones or overtones between 1592 and 1827 cm^{-1}. We note that the intensities of these features are large relative to other phonon modes for vanadium compared to those of the other alums; similar changes in the relative intensities of phonon modes close to eR bands have been noted in the literature.[40,41] Band profile analysis of the eR bands of the rubidium vanadium alums suggest the presence of broad bands at *ca.* 1898 and 2066 cm^{-1}. The relative intensity of the 2066 cm^{-1} band decreases by a factor of *ca.* 2 on cooling to liquid helium temperature, which, given the uncertainties in the temperature of the sample at the scattering point, is consistent with its assignment to ($3\hat{A}_g$, $2\hat{A}_g$) ← $1\hat{E}_g$. The 1898 cm^{-1} band is assigned to $2\hat{E}_g$ ← $1\hat{A}_g$. The relative energies of the SO states shown in Figure 5 suggests a 204 cm^{-1} difference between the energies of the $2\hat{E}_g$ ← $1\hat{A}_g$ and $2\hat{A}_g$ ← $1\hat{E}_g$ transitions, this value representing the upper limit of the separation between the states. The smaller separation observed (168 cm^{-1}) is explained in terms of a reduced SO splitting of the ^3E_g manifold resulting from excited-state J−T effects.

The alternate assignment of the low-wavenumber component of the eR band is to a transition involving excitation from $1\hat{E}_g$, the only candidate being $2\hat{E}_g$ ← $1\hat{E}_g$. This assignment would imply a spread of the SO states resulting from ^3E_g (*ca.* 300 cm^{-1}) much greater than can be explained using crystal field theory, 215 cm^{-1}, this providing an upper estimate of the splitting.

Upon deuteration of the alum, the water bending modes and the combination tones or overtones shift to lower wavenumber and there is a pronounced reduction in the overall half-width of the eR band with the profile dominated by components at *ca.* 1973 and 1828 cm^{-1}. The splitting of 145 cm^{-1} is large compared with that predicted for the $2\hat{E}_g$ ← $1\hat{A}_g$ and $3\hat{E}_g$ ← $1\hat{A}_g$ transitions (110 cm^{-1}), suggesting assignment of the 1973 and 1828 cm^{-1} bands to $2\hat{A}_g$ ← $1\hat{E}_g$ and $2\hat{E}_g$ ← $1\hat{A}_g$, respectively. While these assignments are consistent with analysis of the eR band of the hydrate, it is unclear why there is a shift of the eR band. We were unable to collect the liquid helium spectra of the deuterate which would confirm the assignment of the ground state for the two transitions.

Reports of eR transitions for vanadium(III) in the anhydrous alums[40,41] suggest the presence of preresonant enhancement of the eR band along with unusual polarization properties of the phonon modes. In the present study the phonon modes of the alum lattice are well-defined, and only in the region 1592−1827 cm^{-1} for the hydrates is there any evidence for intensity enhancement. The intensities and polarization properties of the phonon modes outside this range are in keeping with expectations based on other β alums. For excitation wavelengths in the range 406−488 nm there is no evidence of preresonant enhancement of the eR band.

Conclusion

The single-crystal Raman spectra of the rubidium sulfate alums has permitted examination of the dependence of the vibrational frequencies of the internal modes of the $M^{III}O_6$ species with the conformation of the coordinated water molecule and confirmed the classification of the titanium and vanadium rubidium sulfate alums to the β modification. The dimorphism of the rubidium sulfate alums is correlated with the unequal occupancy of the metal(III) t_{2g} (O_h) orbitals. In the cases of titanium and vanadium, electronic factors favor the β over the α modification. The electronic and molecular structures of the tervalent cations may be interpreted within a common framework, where, in cases where the mode of water coordination is trigonal planar, the predominant metal−ligand π interaction is normal to the plane of the water molecule. The trigonal field of the M^{III} site in the alum lattice is dominated by the metal−ligand π interaction, and the magnitude of the trigonal field is much larger for β than α alums. Since the orientation of the plane of the coordinated water molecule is determined by the alum type, and the metal−water π bonding is anisotropic, being greatest normal to the plane of the water molecule, the trigonal field gives orbital singlet and orbital doublet ground terms for vanadium and titanium, respectively. It is our contention that the trigonal field is the dominant interaction so that effects of vibronic and SO coupling should be treated as subsequent perturbations acting within the trigonal manifolds. Evidence of J−T interactions are apparent in the vibrational spectra of the titanium(III) alums and in the electronic Raman spectra of vanadium(III). While comparatively weak in character, the J−T interactions are sufficient to perturb the structural chemistry of the metal hydrates. Further work is in progress directed toward the reinterpretation of the magnetism and EPR spectra of titanium(III) within the framework of this analysis.

Acknowledgment. We thank The Research Corp. Trust for funding of the Oxford Instruments MD4 cryostat and the University of London intercollegiate research service for access to the Raman spectrometer. P.L.W.T.-P. thanks the SERC for the award of a studentship.

IC9602759

(40) Berg, R. W.; Boghosian, S.; Bjerrum, N. J.; Fehrmann, R.; Krebs, B.; Straeter, N.; Mortensen, O. S.; Papatheodorou, G. N. *Inorg. Chem.* **1993,** *32*, 4714−4720.

(41) Fehrmann, R.; Bernt, K.; Papatheodorou, G. N.; Berg, R. W.; Bjerrum, N. J. *Inorg. Chem.* **1986**, *25*, 1571−1577.